

# Viscosity dependence of geminate recombination efficiency after bimolecular charge separation

A. A. Neufeld and A. I. Burshtein

*Department of Chemical Physics, Weizmann Institute of Science, 76100 Rehovot, Israel*

G. Angulo and G. Grampp

*Graz University of Technology, Institute of Physical and Theoretical Chemistry, Graz, Austria*

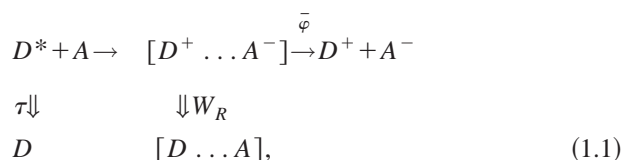
(Received 30 May 2001; accepted 15 November 2001)

The efficiency of geminate recombination after bimolecular ionization of an excited electron donor (or acceptor) is studied. For ions starting from inside or outside the recombination layer, the recombination efficiency has the opposite viscosity dependence. As a result the latter becomes nonmonotonous, provided the kinetic controlled ionization gives way to a diffusional one, creating the more remote ions the higher the solvent viscosity. This effect, first discovered experimentally, receives its explanation here, which is conceivable only on the basis of the Integral Encounter Theory of remote electron transfer in the liquid state. © 2002 American Institute of Physics.

[DOI: 10.1063/1.1433746]

## I. INTRODUCTION

Photoinduced electron transfer reactions play a key role in many chemical and biological processes. After photoexcitation of the electron donor ( $D \rightarrow D^*$ ) or acceptor ( $A \rightarrow A^*$ ), electron transfer between them creates a geminate pair of counterions. In solutions, where the relative distance between reactants is not fixed, but modulated by their stochastic (usually diffusive) motion, these ions may either recombine or be well separated by diffusion. The subsequent bimolecular recombination proceeds during stochastic encounters in a homogeneous solution and usually has a much longer time scale. For instance, the geminate process after photoexcitation of a donor is represented as



where  $[D^+ \dots A^-]$  denotes the geminate ion pair,  $D^+ + A^-$  denotes the pair of ions, well separated by diffusion, while  $[D \dots A]$  represents the ground state of neutral products of geminate recombination. Nothing changes in principle if an initially excited molecule is not a donor, but an acceptor of electrons.

The charge separation quantum yield  $\bar{\phi}$  (average number of the free ions per one photogenerated ion pair) is usually determined from the measurements of the relative quantum yield of fluorescence  $\eta = I/I_0$ , where  $I$  and  $I_0$  are fluorescent intensities with and without quenchers, respectively, and the photoionization quantum yield  $\phi$  (average number of free ions per one absorbed quantum). Then  $\bar{\phi}$  is given by the following relationship

$$\bar{\phi} = \frac{\phi}{1 - \eta}. \quad (1.2)$$

When calculating the quantum yield of geminate charge separation, rather than the kinetics of this process, one may consider the ionization and recombination processes separately. In such a case the irreversible ionization creates an initial ion distribution for the subsequent geminate recombination.<sup>1,2</sup> Thus, in the stationary case, the problem is subdivided into two parts: calculating the distribution of ions created by photoionization,  $f(r_0)$ , and calculating  $\varphi(r_0)$  which is the partial yield of ion separation, provided they started from distance  $r_0$ . The total quantum yield  $\bar{\phi}$  is obtained by averaging the partial one over the distribution of initial separations:

$$\bar{\phi} = \int \varphi(r_0) f(r_0) d^3 r_0. \quad (1.3)$$

Geminate recombination of the ion pairs was the subject of numerous theoretical studies. The main result of these calculations is the partial charge separation yield  $\varphi(r_0)$ . This quantity increases with  $r_0$  and approaches unity at  $r_0 \rightarrow \infty$ . However, in order to calculate the average quantum yield  $\bar{\phi}$ , Eq. (1.3), one needs to know the initial distribution of ions  $f(r_0)$ , which crucially depends on the viscosity of the solution. The reduced characteristics of this distribution is given by the average initial separation

$$\langle r \rangle = \int r f(r) d^3 r \quad (1.4)$$

which logarithmically increases with viscosity.<sup>3</sup> However, such a reduction is not well suited, as it will be shown in Sec. IV. Therefore, we employ the Integral Encounter Theory (IET), which provides the most efficient way for a straightforward calculation of the charge separation quantum yield. Besides, IET keeps Eq. (1.3) valid (see Sec. IV), which simplifies the qualitative interpretation of the results obtained.

Usually the charge separation quantum yield is represented by the ratio of recombination efficiency  $Z$  and the encounter diffusion coefficient of counterions  $\tilde{D}$ :

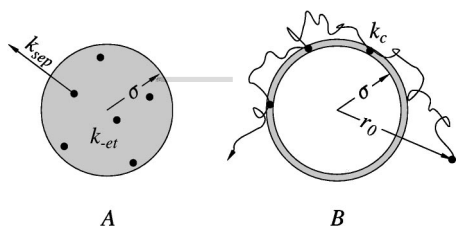


FIG. 1. The schematic representation of the exponential model (EM) and contact approximation (CA). In EM the reaction sphere of radius  $\sigma$  is transparent for particles, which leave it by a single jump. In CA the same sphere is an excluded volume and recombination takes place only at its surface, when it is touched.

$$\bar{\varphi} = \frac{1}{1 + Z/\bar{D}}. \quad (1.5)$$

According to the primitive but popular “Exponential Model” (EM), the uniform recombination rate  $k_{-et}$  competes with the rate of diffusional separation from spherical reaction zone  $k_{sep} \propto \bar{D}$  [see Fig. 1(a)], so that the expectation of EM is invariable  $Z \propto k_{-et} = \text{const}$ . In the more sophisticated contact or rectangular approximations of the reaction zone the recombination efficiency  $Z$  depends on diffusion. However, this dependence is either ascending or descending, but never passes through the maximum that appears in our experiments at a certain viscosity (Fig. 2). The explanation for this extremum observed in a system of perylene (donor) with *N,N*-dimethylaniline is the main goal of the present article. This is actually the first experimental indication that highly exergonic backward electron transfer is never contact, while

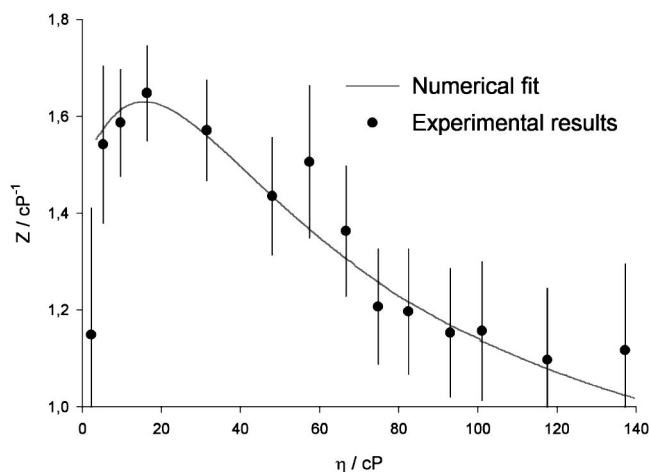


FIG. 2. The experimentally measured viscosity dependence of the recombination efficiency  $Z$  in the reaction of the electron transfer quenching of perylene by *N,N*-dimethylaniline (DMA). The mixtures of dimethylsulfoxide (DMSO) with glycerol were used to change the viscosity of the solvent. Excitation energy of perylene  $\mathcal{E} = 2.83$  eV,  $\Delta G_i = -0.56$  eV,  $\Delta G_r = -2.27$  eV, the solvent (outer-sphere) reorganization energy is  $\lambda_0 = 0.885$  eV,  $L = 1 \text{ \AA}$ ,  $\tau = 4.3$  ns. The theoretical fit (solid line) was done with  $w_i = 230 \text{ ns}^{-1}$ ,  $\lambda_i = 0.1298$  eV for ionization and  $w_r = 1320 \text{ 1/ns}$ ,  $\lambda_i = 0.2346$  eV for recombination that was considered as multichannel (phonon assisted) transfer with vibronic quantum mode  $\omega = 43.510 \cdot 10^{-3}$  eV and corresponding reorganization energy 0.608 49 eV (these parameters were taken from Ref. 4).

the forward transfer changes from remote to contact, as the encounter diffusion of neutral reactants speeds up.

The outline of this article is the following. Section II summarizes the results of some model calculations of  $Z$  for ions initially separated by distance  $r_0$ . In Sec. III the Integral Encounter Theory (IET) is used for the calculation of the charge separation quantum yield. An analysis of the distance dependence of the Marcus electron transfer rates is also presented there, especially for the highly excited donor. The viscosity dependence of the recombination efficiency is analyzed in Sec. IV. It is shown, that at sufficiently high exergonicity of recombination its efficiency may have a maximum in the viscosity dependence conditioned by the change in the initial distribution of ions at increasing viscosity. However, the fit of the whole experimental data by the numerical calculations, based on IET, will be postponed until our next paper, which accounts for the few additional factors affecting ion recombination.

## II. RECOMBINATION EFFICIENCY

A pair of counterions  $[D^+ \dots A^-]$ , initially separated by a small distance  $r_0$ , can either recombine to the ground state of neutral products  $[D \dots A]$ , or be well separated with characteristic time, related to the solvent viscosity. In the following, we discuss two different models, allowing for the analytic calculation of the partial charge separation yield  $\varphi(r_0)$ . They are the contact and rectangular approximations of the recombination layer.

### A. Contact approximation

The earliest consistent model of the phenomenon, allowing for an analytic solution, was the contact approximation for the rate of recombination. In such an approximation the actual recombination rate  $W_R(r)$  is replaced by a  $\delta$ -function, at a distance of the closest approach  $\sigma$  [see Fig. 1(b)], i.e.,

$$W_R(r) \approx k_c \frac{\delta(r - \sigma)}{4\pi r \sigma}, \quad k_c = \int W_R(r) d^3r. \quad (2.1)$$

The relative motion of ions is treated as diffusion in a Coulomb well with Onsager radius  $r_c$ . Note, that the  $\delta$ -function approximation, Eq. (2.1), may alternatively be introduced by appropriate change in the boundary condition at the distance of closest approach.

In the contact approximation the partial charge separation yield depends on the diffusion coefficient and starting distance  $r_0$ :<sup>5-9</sup>

$$\varphi(r_0) = \frac{1}{1 + Z(r_0; \bar{D})/\bar{D}}, \quad (2.2)$$

as well as the corresponding recombination efficiency:

$$Z(r_0; \bar{D}) = \frac{q(r_0)z}{1 + [1 - q(r_0)]z/\bar{D}}. \quad (2.3)$$

Here

$$z = \frac{k_c}{4\pi r_c} [e^{r_c/\sigma} - 1], \quad (2.4)$$

where  $r_c$  is the Onsager radius of the Coulombic attraction and

$$q(r_0) = \frac{1 - \exp(-r_c/r_0)}{1 - \exp(-r_c/\sigma)} \leq 1, \quad q(\sigma) = 1. \quad (2.5)$$

Note, that the recombination efficiency is independent of the diffusion only for ions, created at contact distance  $r_0 = \sigma$ :  $Z(\sigma) = z = \text{const.}$

At any  $r_0 > \sigma$  the recombination efficiency  $Z(r_0; \bar{D})$ , defined by Eqs. (2.3)–(2.5), monotonously increases with an increase in the diffusion coefficient  $\bar{D}$  (or with a decrease in the solvent viscosity) and approaches the plateau  $q(r_0)z$ . This allows subdividing the geminate reactions into the same classes, as bimolecular ones: diffusion and kinetic controlled. The former case appears at slow diffusion and only for the noncontact creation of ions  $r_0 > \sigma$ , while in the opposite limit the recombination efficiency does not depend on diffusion and is smaller, the larger the initial separation of ions  $r_0$ ,

$$Z(r_0; \bar{D}) = \begin{cases} \frac{q(r_0)\bar{D}}{1 - q(r_0)} & \text{diffusional} \quad \bar{D} \ll [1 - q(r_0)]z \\ q(r_0)z & \text{kinetic} \quad \bar{D} \gg [1 - q(r_0)]z. \end{cases} \quad (2.6)$$

Diffusion acceleration of the recombination efficiency was observed in the reaction of Ru-tris(2,2'-bipyridine), Ru(bipy)<sub>3</sub><sup>2+</sup>, with methylviologen, MV<sup>2+</sup>, studied in Ref. 10. It was considered in Ref. 11 and later<sup>2</sup> as a manifestation of the noncontact creation of ions. However, the theory ignoring the spin states of ions, failed to reproduce the nonlinear dependence of the recombination efficiency on viscosity, observed experimentally in Ref. 10. Later on, it was attributed to a spin conversion in the ion pair, which controls its recombination from initially created triplet state to a singlet ground state of the products.<sup>12–14</sup>

It should be stressed that the contact approximation is applicable only if the initial separation  $r_0$  sufficiently exceeds the external radius of the recombination layer. This is possible only under the diffusional control of the forward electron transfer, which creates radical ions farther from each other, the slower the diffusion of the reactants. This is not quite clear whether this condition is satisfied in the case of reactions studied in Ref. 10. If this condition is not met and the forward electron transfer is under kinetic control, then its products are located near the contact. In such a case the rectangular approximation of  $W_R(r)$  should be better employed instead of the contact one. The rectangular model of the recombination layer allows the exact analytic solution for ions starting from either the exteriority or interior of this layer.<sup>15</sup>

## B. Rectangular model of the remote reaction layer

The rectangular approximation of the recombination rate is introduced as

TABLE I. Recombination efficiency vs separation.

	$Z(r_0; \bar{D})$	$r_0$
A	$\frac{z[\cosh(\xi L) + \xi r_1 \sinh(\xi L) - 1]}{\xi^2 L R}$	$\sigma \leq r_0 \leq r_1$
B	$\frac{\xi r_0 [e^{\xi L} - \kappa e^{-\xi L}]}{e^{\xi(r_0 - r_1)} + \kappa e^{-\xi(r_0 - r_1)}} - 1$	$r_1 \leq r_0 \leq r_2$
C	$\frac{r_2}{r_0} \frac{z}{1 + [1 - r_2/r_0]\xi^2 L R}$	$r_2 \leq r_0$

$$W_R(r) = \begin{cases} 0 & \sigma \leq r < r_1 \\ W_0 & r_1 \leq r \leq r_2 \\ 0 & r_2 < r. \end{cases} \quad (2.7)$$

The exact analytic solution, obtained in Ref. 15 for highly polar solvents ( $r_c = 0$ ), predicts a different viscosity dependence of the recombination efficiency  $Z(r_0; \bar{D})$ , at a different initial separation of ions.

In Table I  $L = r_2 - r_1$  is the width of the rectangular reaction layer,  $R = r_1 + L/2$ ,  $\xi = \sqrt{W_0/\bar{D}}$ , and  $\kappa = (\xi r_1 - 1)/(\xi r_1 + 1)$ . The parameter of the kinetic recombination

$$z = W_0 L r_1 \quad (2.8)$$

coincides with that which follows from Eq. (2.4) at  $r_c = 0$ , provided the contact approximation is valid:  $r_1 = \sigma$ ,  $L \rightarrow 0$ . For this very case Eq. (2.1) gives  $k_c \approx 4\pi\sigma^2 L W_0$ .

Figure 3 shows the recombination efficiency at different initial separations, indicated in the figure, as a function of viscosity, measured by the mean encounter time for neutral reactants  $\tau_d = \sigma^2/\bar{D}$ . The rectangular approximation of the real recombination layer, used in our calculations, is shown by the dotted line on Fig. 4(a). For ions, starting from inside this layer, the recombination efficiency increases with increasing viscosity and does not depend on the initial separation  $r_0$  until it is less than  $r_1$  (two upper curves in Fig. 3).

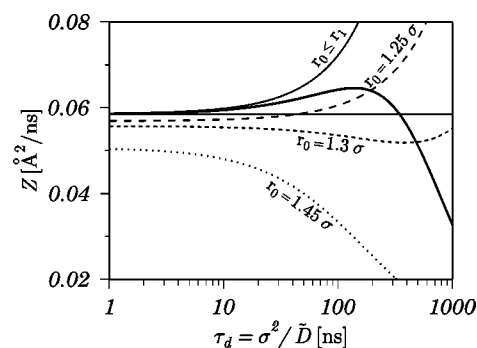


FIG. 3. The viscosity dependence of the recombination efficiency  $Z(r_0; \bar{D})$  at fixed starts from contact region (thin solid line), from inside the remote recombination layer (long dashed and dashed lines) and outside of it (dotted line). The corresponding initial separations are indicated in the figure. The true  $Z(\bar{D})$  dependence, calculated via the average quantum yield  $\bar{\varphi}$ , Eq. (2.10), is indicated by the thick solid line. The parameters, defining rectangular recombination layer:  $r_1 = 1.1\sigma$ ,  $r_2 = 1.4\sigma$ ,  $W_0 = 0.156 \text{ ns}^{-1}$  ( $\sigma = 10\text{Å}$ ). The horizontal line represent  $z = 0.0585 \text{ Å}^2/\text{ns}$ , Eq. (2.8). The parameters, defining the ionization layer, and used to calculate the average quantum yield, are indicated in Fig. 4(A).

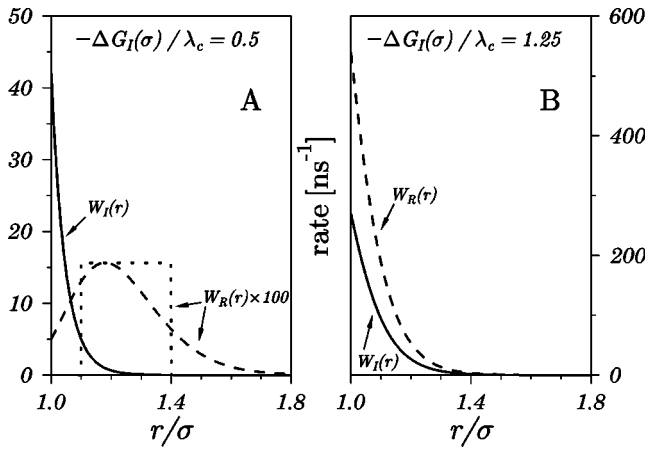


FIG. 4. The shape of the ionization (solid lines) and recombination (dashed lines) rates in (A) NI subregion,  $-\Delta G_I(\sigma) = 0.5 \lambda_c$ ,  $-\Delta G_R(\sigma) = 2.0 \lambda_c$ , and (B) II—subregion,  $-\Delta G_I(\sigma) = -\Delta G_r = 1.25 \lambda_c$ . The pre-exponential factors, Eq. (3.13), are  $w_I = 500 \text{ ns}^{-1}$ ,  $w_R = 1000 \text{ ns}^{-1}$ ; the space decrement of electron tunneling  $L/\sigma = 0.142$  ( $\sigma = 10 \text{ \AA}$ ), outer-sphere reorganization energy  $\lambda_c = 1 \text{ eV}$ . The highly polar solvent ( $r_c = 0$ ), and room temperature ( $T = 293 \text{ K}$ ).

This effect is attributed to an increase in the residence time in the reaction layer, which makes recombination inside it more efficient. The opposite, descending dependence of  $Z$  on viscosity is observed for outer starts. At a sufficiently large initial separation  $r_0$ , the recombination efficiency is well estimated by the contact approximation formulas, Eqs. (2.3)–(2.5), setting

$$k_c = \int W_R(r) d^3 r = W_0 \cdot \frac{4}{3} \pi (r_2^3 - r_1^3). \quad (2.9)$$

The result is identical to Eq. (2.6). At high viscosities the reaction is controlled by diffusion and the recombination efficiency is reduced when diffusion slows down (the lowest curve in Fig. 3).

Thus, the recombination efficiency parameter  $Z(r_0; \bar{D})$  has the opposite viscosity dependence for ions, starting from inside and outside the reaction layer. The mixed situation takes place in between, when ions start from behind the outer border of the reaction layer: the viscosity dependence of the recombination efficiency may have a minimum, the short-dashed line in Fig. 3. However, the average quantum yield  $\bar{\varphi}$  available experimentally, accumulates all these opportunities, as well as the true recombination efficiency

$$Z(\bar{D}) = \bar{D} \left[ \frac{1}{\bar{\varphi}} - 1 \right]. \quad (2.10)$$

As a result the viscosity dependence of  $Z(\bar{D})$  is essentially affected by the shape of the initial ion distribution which also changes with viscosity. The high sensitivity of the results to the shape of the functions, subject to convolution in Eq. (1.3), makes undesirable any simplification of them. On the other hand, the average charge separation quantum yield is available for the exact numerical calculations by means of the efficient and convenient integral encounter theory, which is formulated in the following section.

### III. INTEGRAL ENCOUNTER THEORY

The IET is the modest version of Encounter Theory that proved to be very profitable in studying a number of applications including those which are prohibitive for conventional rate description. The fresh review of the progress that IET made during last decade is given in Ref. 16. The newest version of IET is given in matrix formulation<sup>17</sup> which allows to consider as many stages and reactants as really compose a complex reaction in liquid solution. However, for the present goal it is enough to use one of the earliest and simplest formulations of IET given in Ref. 18.

The irreversible ionization, followed by geminate charge recombination, is described by a reduced set of IET equations where the bimolecular recombination of ions in the bulk is neglected. These equations describe the short time evolution of the system after instantaneous excitation:<sup>18</sup>

$$\dot{P}^*(t) = -c \int_0^t R^*(\tau) P^*(t-\tau) d\tau - \frac{P^*(t)}{\tau}, \quad (3.1)$$

$$\dot{P}^\dagger(t) = c \int_0^t R^\dagger(\tau) P^*(t-\tau) .d\tau. \quad (3.2)$$

Here  $c$  is the concentration of quenchers present in great excess,  $P^*(t)$  is the survival probability of excitation,  $P^\dagger(t) = [D^+] = [A^-]$  is that for ions,  $R^*(\tau)$  and  $R^\dagger(\tau)$  are the IET kernels (memory functions). Initially  $P^*(0) = 1$  and  $P^\dagger(0) = 0$ , but as  $t \rightarrow \infty$  excitations disappear ( $P^*(\infty) = 0$ ), while the charge concentration levels off indicating the photoionization (free ion) quantum yield,

$$P^\dagger(\infty) = \phi = \psi \bar{\varphi}. \quad (3.3)$$

Here

$$\psi = 1 - \eta = \frac{c \bar{R}^*(0) \tau}{1 + c \bar{R}^*(0) \tau} \quad (3.4)$$

is the total quantum yield of ions while charge separation quantum yield

$$\bar{\varphi} = \bar{R}^\dagger(0) / \bar{R}^*(0) \quad (3.5)$$

equals the fraction of them which escaped geminate recombination.<sup>18</sup> In the next section it will be shown, that Eq. (3.5) may be represented in the form of Eq. (1.3).

Thus, within the framework of IET all the quantities of interest are expressed via the Laplace transformed kernels:

$$\bar{R}^{*,\dagger}(s) = \int_0^\infty R^{*,\dagger}(t) e^{-st} dt, \quad (3.6)$$

for argument  $s = 0$ . These kernels are different:  $\bar{R}^*$  accounts solely for the irreversible ionization, while  $\bar{R}^\dagger$ , in addition, takes into account the recombination into the ground state:

$$\bar{R}^*(s) = \left[ s + \frac{1}{\tau} \right] \int W_I(r) \tilde{\nu}(r; s) d^3 r \quad (3.7)$$

$$\bar{R}^\dagger(s) = \bar{R}^*(s) - \left[ s + \frac{1}{\tau} \right] \int W_R(r) \tilde{\mu}(r; s) d^3 r. \quad (3.8)$$

The Laplace transformed pair correlation functions  $\tilde{v}(r;s)$  and  $\tilde{\mu}(r;s)$  obey the following auxiliary equations<sup>18</sup>

$$\left[ s + W_I(r) + \mathcal{L}_r + \frac{1}{\tau} \right] \tilde{v}(r;s) = 1, \quad (3.9a)$$

$$[s + W_R(r) + \mathcal{L}_r^c] \tilde{\mu}(r;s) = W_I(r) \tilde{v}(r;s), \quad (3.9b)$$

with the reflective boundary conditions at the distance of closest approach,  $\sigma$ . Here  $\tau$  is the lifetime of the excited donor, while the linear operators

$$\mathcal{L}_r = \frac{1}{r^2} \frac{\partial}{\partial r} r^2 D(r) \frac{\partial}{\partial r} \quad (3.10a)$$

$$\mathcal{L}_r^c = \frac{1}{r^2} \frac{\partial}{\partial r} r^2 \tilde{D}(r) \left( \frac{\partial}{\partial r} + \frac{1}{T} \frac{dU(r)}{dr} \right) \quad (3.10b)$$

define the relative motion of neutral reactants and ions, respectively. In our model the motion is diffusive with the distant dependent encounter diffusion coefficients for neutral and charged reactants,  $D$  and  $\tilde{D}$ .  $U(r)$  in Eq. (3.10b) is the potential of the external forces (the Boltzmann constant  $k_B = 1$ , and thus the absolute temperature  $T$  is measured in units of energy). For the nonscreened Coulomb attraction one has, for instance,

$$\frac{U(r)}{T} = -\frac{r_c}{r}, \quad (3.11)$$

where  $r_c = e^2/(\epsilon T)$  is the Onsager radius, which is expressed via the elementary charge  $e$  and dielectric constant of the medium  $\epsilon$ .

Our numerical approach to the calculation of the charge separation quantum yield  $\bar{\varphi}$  is based on Eqs. (3.5)–(3.10), and we need to specify the explicit form of the distance dependence of the rates of the forward and backward electron transfer,  $W_I(r)$  and  $W_R(r)$ . In the simplest case of the single-channel electron transfer, these rates introduced have the following Marcus' form:<sup>19,2</sup>

$$W(r) = w \sqrt{\frac{\lambda_c}{\lambda(r)}} e^{-2(r-\sigma)/L} \times \exp \left[ -\frac{[\Delta G(r) + \lambda(r)]^2}{4\lambda(r)T} \right], \quad (3.12)$$

where

$$w = \frac{\sqrt{\pi} V_0^2}{\sqrt{\lambda_c T}}. \quad (3.13)$$

Here  $V_0$  and  $L$  are matrix elements and the length of electron tunneling, while  $\lambda(r)$  is the distance dependent reorganization energy,

$$\lambda(r) = \lambda_i + \lambda_o \left( 2 - \frac{\sigma}{r} \right), \quad (3.14)$$

composed from the intramolecular contribution ( $\lambda_i$ ) and the “outer-sphere” (medium) part,

$$\lambda_o = e^2 \gamma \left( \frac{1}{2r_A} + \frac{1}{2r_D} - \frac{1}{\sigma} \right). \quad (3.15)$$

Here  $r_A$  and  $r_D$  are the radii of the acceptor and donor, respectively, and

$$\gamma = \frac{1}{n^2} - \frac{1}{\epsilon} \quad (3.16)$$

is the so-called Pekar's factor, being determined by the medium refraction index  $n$  and the dielectric constant  $\epsilon$ .

The positions and shapes of the reaction layers for the recombination and ionization are determined by their exergonicities at contact,  $\Delta G_{i,r} = \Delta G_{I,R}(\sigma)$ , and contact reorganization energy  $\lambda_c = \lambda(\sigma) = \lambda_i + \lambda_o$ .<sup>20,2</sup> The sum of the free energies of the backward and forward electron transfer is fixed by the constant energy of photoexcitation  $\mathcal{E}$ :

$$\Delta G_I(r) + \Delta G_R(r) = -\mathcal{E}. \quad (3.17)$$

For the backward electron transfer the free energy is

$$\Delta G_R(r) = \Delta G_r + T \left( \frac{r_c}{\sigma} - \frac{r_c}{r} \right), \quad (3.18)$$

while that for forward transfer,  $\Delta G_I(r)$ , is readily determined from Eqs. (3.17)–(3.18). If  $-\Delta G(\sigma) < \lambda_c$ , then the transfer occurs in the so-called Marcus normal region, and the corresponding rate  $W(r)$  monotonously decreases with the increase in the relative distance between reactants. In the opposite situation  $W(r)$  has a bell shape with the maximum shifted out of contact, the more the larger is  $-\Delta G(\sigma) > \lambda_c$ . Thus, the type of transfer rates entirely depends on the relative values of the contact free energies. If  $|\Delta G_i|$  increases with replacing the electron acceptor, then  $|\Delta G_r|$  decreases and vice versa, since the sum of them is fixed by Eq. (3.17). As it was shown in Ref. 21, one should discriminate between three different situations:  $\mathcal{E} < 2\lambda_c$ ,  $\mathcal{E} = 2\lambda_c$  and  $\mathcal{E} > 2\lambda_c$ . The borderline situation  $\mathcal{E} = 2\lambda_c$  was rigorously studied in Ref. 21. In the present article we concentrate on the case of a fairly high excitation energy  $\mathcal{E} > 2\lambda_c$ .

Figure 5 shows the contact values of the ionization and recombination rates for  $\mathcal{E} = 2.5\lambda_c$ . This figure can be divided in two equal parts. In the left half, ionization is less exergonic than recombination, while in the right half the situation is the opposite. As a result, in the former case the ionization layer is located inside the recombination one, while in the latter they interchange their positions (see their schematic representation at the bottom of Fig. 5).

When ions are generated outside the recombination layer, one should expect the monotonous decrease of the recombination efficiency  $Z$ , with increasing viscosity, which hinders delivery of remote ions to the inner recombination zone. However, in this case the highly exergonic photoionization can hardly compete with thermal ionization and therefore is worse suited for experimental study in the large free energy region.

The more abundant is the opposite situation which allows for the generation of ions inside the recombination layer. At fast diffusion, when ionization is under kinetic control the initial distribution of ions  $f(r_0)$  reproduces the shape

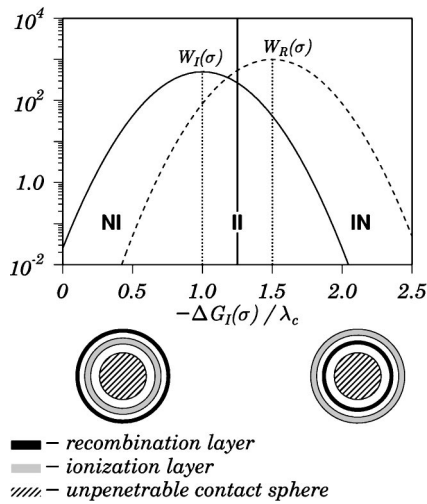


FIG. 5. The separation of different regions of the forward and backward electron transfer at  $\mathcal{E}=2.5 \lambda_c$ . In the left half the ionization layer is positioned inside that of recombination (shaded in the bottom scheme). In the right half vice versa. These main regions are subdivided into the more narrow NI (normal ionization, inverted recombination), II (both reactions occur in inverted regions) and IN (inverted ionization, normal recombination). The parameters are the same, as for Fig. 4.

of the ionization rate,  $W_I(r)$ . In this case  $Z$  is expected to increase with viscosity, which prolongs the ion residence in the recombination layer that should be crossed on their way out. At higher viscosities when the kinetic control gives way to the diffusional one, the actual ionization may occur at the outer periphery of the ionization layer, and even outside the recombination layer, as in the previous case.

This is a distinctive feature of the phenomenon not studied earlier: the initial conditions for recombination are varied with the viscosity of the solution. When the viscosity increases, the initial ion distribution  $f(r_0)$  is shifted out of contact, acquires a bell shape and at least its wing shows itself outside the recombination layer (see Fig. 6). This proves to be sufficient to provide the maximum in the viscosity dependence of the true recombination efficiency,  $Z(\bar{D})$ . Initially  $Z$  increases, approaches a maximum and only then decreases with viscosity. In the following section the above statement will be discussed in more detail on the basis of the exact numerical calculations.

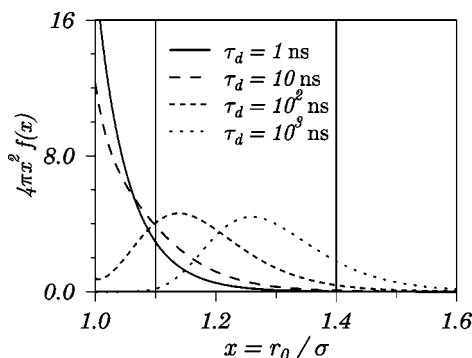


FIG. 6. The normalized distributions  $f(r_0)$  over the initial ions separation at different values of viscosity, indicated in the figure. The other parameters, defining the ionization layer, are the same as for Fig. 4.

#### IV. INITIAL ION DISTRIBUTION

In the unified theory<sup>2</sup> the charge separation quantum yield after irreversible photoionization,  $\bar{\varphi}$ , was given by the expression (1.3), which is the average of the partial separation yield  $\varphi(r_0)$  over the initial distribution of ions  $f(r_0)$ . This important recipe of the charge separation quantum yield calculation remains valid in IET as well, although both multipliers under the integral in Eq. (1.3) have a bit of difference in definitions.

Making the substitution of kernels (3.7) and (3.8) at  $s = 0$  into Eq. (3.5), one has

$$\bar{\varphi} = 1 - \frac{\int W_R(r) \tilde{\mu}(r;0) d^3r}{\int W_I(r) \tilde{\nu}(r;0) d^3r}. \quad (4.1)$$

The solution of Eq. (3.9b) establishes the relationship between two pair distributions:

$$\tilde{\mu}(r;0) = \int \tilde{G}(r,r_0;0) W_I(r_0) \tilde{\nu}(r_0;0) d^3r_0. \quad (4.2)$$

The Green function of ions subjected to geminate recombination,  $\tilde{G}(r,r_0;s)$ , obeys the following equation:

$$[s + W_R(r) + \mathcal{L}_r^c] \tilde{G}(r,r_0;s) = \frac{\delta(r-r_0)}{4\pi r r_0}. \quad (4.3)$$

The reflective boundary condition should be used with this equation, the same as with Eq. (3.9).

On substitution of Eq. (4.2) into Eq. (4.1), it is readily seen, that the latter can be written in the form of Eq. (1.3), where the partial separation yield of ions is

$$\varphi(r_0) = 1 - \int W_R(r) \tilde{G}(r,r_0;0) d^3r, \quad (4.4)$$

and their normalized initial distribution is given by the IET formula:<sup>22</sup>

$$f(r_0) = \frac{W_I(r_0) \tilde{\nu}(r_0;0)}{\int W_I(r) \tilde{\nu}(r;0) d^3r}. \quad (4.5)$$

At fast diffusion, when ionization is under kinetic control, this distribution reproduces the shape of  $W_I(r)$ , but moves away, when the viscosity increases and ionization becomes diffusion controlled.<sup>2,3</sup> The transformation of these distributions with increasing viscosity is shown in Fig. 6. Hence, at the lowest viscosity ions start mainly from inside the remote recombination layer, while at higher viscosity they also start from outside.

#### V. DISCUSSION

The most common simplification of the initial distribution  $f(r)$  is its reduction to a  $\delta$ -function, located at a given initial distance between the ions,  $r_0$ :

$$f(r) \approx \frac{\delta(r-r_0)}{4\pi r_0^2}. \quad (5.1)$$

As a result the average quantum yield  $\bar{\varphi}$  is also reduced to the partial separation yield of ions, starting from this very distance,  $r_0$ :

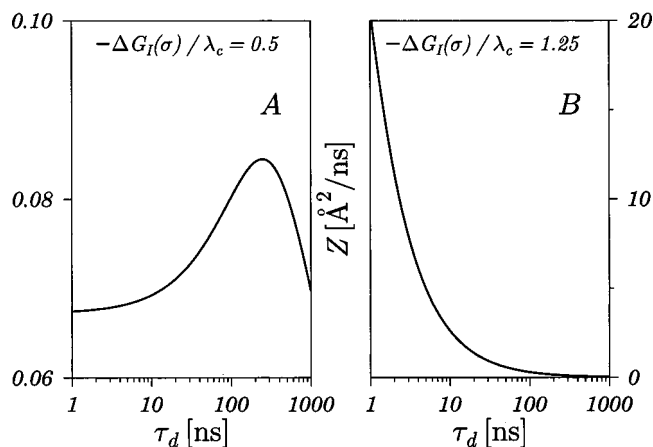


FIG. 7. The viscosity dependence of the recombination efficiency  $Z(\bar{D})$  for the Marcus-type rates of ionization and recombination, Eq. (3.12). All the parameters are the same as for Fig. 4. The viscosity is measured by the mean encounter time for the neutral reactants  $\tau_d = \sigma^2/\bar{D}$ . The excitation energy of the donor  $\mathcal{E} = 2.5 \lambda_c$ .

$$\bar{\varphi} \rightarrow \varphi(r_0). \quad (5.2)$$

It seems reasonable to choose  $r_0$  equal to the average initial separation, Eq. (1.4). This approximation shows the right tendency: the start from inside the recombination zone is changed by a start from outside, since  $r_0 = \langle r \rangle$  increases monotonously at increasing viscosity. Nevertheless, such an approximation proves to be too rough, because the real initial distribution is not pointlike, but very broad. Part of it is covered by the recombination zone, while another part appears outside it (Fig. 6). When the residence time in the recombination zone is sufficiently large, the inner starts (for which ions inevitably cross the recombination layer) contributes to the charge separation yield  $\bar{\varphi}$ , much less than the outer starts (for which ions may avoid the recombination layer at all). This happens despite the fact, that only the far wing of  $f(r_0)$  shows itself outside the recombination layer. As soon as this wing starts to dominate,  $Z$  falls down with further increase of viscosity. In the opposite situation of fast diffusion, the contribution of the far wing is negligible, while the ion started from the interior of the recombination contributes more to  $Z$  when the viscosity increases.

Hence, the maximum in the viscosity dependence of  $Z$  indicates equilibration of inner and outer start contributions into the charge separation yield, as well as in the recombination efficiency. The maximum depends not only on the position of the initial distribution regarding the reaction layer, but also on the strength of the recombination and the width of the layer which determines the residence time in there.

Thus, it is much better to account for the real initial ion distribution  $f(r_0)$ , instead of its  $\delta$ -function approximation, and to use the true recombination rate  $W_R(r)$ , instead of its rectangular model. It may be done on the basis of the exact numerical solution of the IET equations. The results obtained with the particular reaction rates of the electron transfer, indicated on Fig. 4 are represented in Fig. 7. In NI case A the remote recombination layer is shifted far away from the quasi-contact ionization layer, while in II case B both for-

ward and backward transfers are in inverted region having exactly the same free energies ( $\Delta G_I(\sigma) = \Delta G_R(\sigma)$ ) so that the shapes of both layers are identical. Correspondingly, the recombination efficiency parameter  $Z(\bar{D})$  has a well pronounced maximum in the former case, while in the latter one can see only the monotonous decrease of recombination efficiency with increasing viscosity. This is because at any finite diffusion the initial ion distribution is wider than ionization layer, and hence, aligned mainly outside both reaction layers of the same shape and width. Even stronger separation is inherent to IN case when the recombination layer is located nearer to contact, deeply inside ionization one and corresponding initial distribution of ions.

Only the monotonous increase of  $Z$  with  $\bar{D}$ , peculiar to case B, was experimentally observed until now<sup>10</sup> and subjected to the theoretical description in a number of works.<sup>11–14</sup> However, in (Fig. 2) we have demonstrated the fresh experimental evidence of the nonmonotonous  $Z(\bar{D})$  behavior, typical for case A. The system studied experimentally is the electron transfer quenching of perylene (Per) by N,N-dimethylaniline (DMA), which has been widely used.<sup>23</sup> This process is characterized by the high excitation energy of the electron acceptor (Per,  $\mathcal{E} = 2.83$  eV), ionization in the Marcus normal region ( $\Delta G_i = -0.55$  eV) and highly exergonic recombination proceeding in the Marcus inverted region,  $\Delta G_r = -2.28$  eV.

The special measures were undertaken to get the maximum located inside the available range of the viscosity variation. This variation should not be accompanied by the changing of any of the other physical properties of the solvent. To meet this requirement in the fairly wide viscosity range the dimethylsulfoxide (DMSO)-glycerol mixtures were used. These mixtures show almost a constant refraction index, as well as a similar and high dielectric constant. Perylene (Aldrich, 99.5%), glycerol (Aldrich 99.8%, <0.1% H<sub>2</sub>O) were used as received. DMA (Aldrich, >99%) was distilled under reduced pressure (17 mbar, 77 °C) and always handled under argon. DMSO (Fluka, 0.05% H<sub>2</sub>O) was twice crystallized by freezing cycles.<sup>24</sup> The concentrations of perylene,  $2 \times 10^{-5}$  M, and of the DMA, 0.033 M, were kept constant throughout all the laser flash photolysis experiments. Absorption, emission, and lifetime equipments used, have already been described.<sup>25</sup> After the laser experiments the kinematic viscosities were determined using a thermostated Ubbelohde viscosimeter. All the measurements were done setting the temperature at  $20.0 \pm 0.1$  °C. A more detailed outline of the experimental technique will be given elsewhere.

Several additional factors have to be taken into account when fitting the experimental data, like the multiphonon character of the electron transfer in the Marcus inverted region, singlet-triplet conversion in the ions pair, etc. This will be done in our next article. However, we would like to stress that the nonmonotonous viscosity dependence of the recombination efficiency, Fig. 2, may be considered as the true one, rather than due to the collateral modulation of the reorganization energy and Coulombic forces, which may occur in some other mixtures.

## VI. CONCLUSIONS

The viscosity dependence of the charge separation quantum yield was studied a few times theoretically, within the exactly solvable models, assuming the initial separation of ions is given. For the narrow recombination layer adjacent to contact, the distant starts are implied, while for the remote recombination layer not only are outer starts possible, but they are also possible from the interior of the reaction zone. The former situation was studied with the conventional contact approximation, while the latter requires rectangular simplification of the recombination rate shape.<sup>2</sup> In any case only the recombination assisted by diffusion was under investigation, but not the influence of the initial ion separation which is also affected by diffusion.

The distinctive feature of the present work is a proper account of the initial ion separation which is not the fitting parameter and changes with solvent viscosity. In fact, this is not a single distance in a pair, but a distribution of distances produced by a precursor bimolecular electron transfer (ionization). At large viscosity this reaction is controlled by diffusion and all starts are distant. In less viscous solvents the distribution of starting distances shifts to contact and under kinetic control coincides in form with the ionization rate. In the latter case ions generated near the contact appear deeply inside the recombination layer provided the backward transfer is highly exergonic and therefore remote.

The interchange in the positions of the initial ion distribution and recombination layer is responsible for the nonmonotonous viscosity dependence of the recombination efficiency which increases with viscosity for inner starts and decreases for outer ones. This main conclusion of the integral encounter theory is qualitatively confirmed by an experimental study of the system with a highly variable viscosity. The efficient programs for solving integral equations which are developed and used here, proved to be suitable for a quantitative fitting of the theory to the experimental data shown in Fig. 2. A more detailed and complete work accounting for spin conversion in the ion pair and parallel recombination of them to the triplet state of the products is now in progress.

## ACKNOWLEDGMENTS

This work was supported by the Israeli Science Foundation (Project N 6863). The authors (G.A. and G.G.) would like to thank the Austrian National Bank, Austrian Exchange Service (AD), TU Graz, and VW-Foundation (Germany) for financial support.

- <sup>1</sup>A. I. Burshtein, Chem. Phys. Lett. **194**, 247 (1992).
- <sup>2</sup>A. I. Burshtein, Adv. Chem. Phys. **114**, 419 (2000).
- <sup>3</sup>A. I. Burshtein, E. Krissinel, and M. S. Mikhelashvili, J. Phys. Chem. **98**, 7319 (1994).
- <sup>4</sup>A. I. Burshtein and A. Yu. Sivachenko, Chem. Phys. **235**, 257 (1998).
- <sup>5</sup>R. J. Harrison, B. Pears, G. S. Beddard, J. A. Cowan, and J. K. M. Sanders, Chem. Phys. **116**, 429 (1987).
- <sup>6</sup>I. R. Gould, J. E. Mozer, D. Ege, and S. Farid, JACS **110**, 1991 (1998).
- <sup>7</sup>G. Grampp and G. Hetz, Ber. Bunsenges. Phys. Chem. **96**, 198 (1992).
- <sup>8</sup>K. M. Hong and J. Noolandi, J. Chem. Phys. **68**, 5163 (1978).
- <sup>9</sup>A. I. Burshtein, A. A. Zharikov, N. V. Shokhirev, O. B. Spirina, and E. B. Krissinel, J. Chem. Phys. **95**, 8013 (1991).
- <sup>10</sup>H.-J. Wolff, D. Bürßner, and U. Steiner, Pure Appl. Chem. **67**(1), 167 (1995).
- <sup>11</sup>A. I. Burshtein, J. Chem. Phys. **103**, 7927 (1995).
- <sup>12</sup>A. I. Burshtein and E. B. Krissinel, J. Phys. Chem. A **102**, 816 (1998).
- <sup>13</sup>E. B. Krissinel, A. I. Burshtein, N. N. Lukzen, and U. Steiner, Mol. Phys. **96**, 1083 (1999).
- <sup>14</sup>A. I. Burshtein, E. B. Krissinel, and U. Steiner, PCCP **3**, 198 (2001).
- <sup>15</sup>A. I. Burshtein and N. V. Shokhirev, J. Phys. Chem. A **101**, 25 (1997).
- <sup>16</sup>A. I. Burshtein, J. Lumin. **93**, 229 (2001).
- <sup>17</sup>K. L. Ivanov, N. N. Lukzen, A. B. Doktorov, and A. I. Burshtein, J. Chem. Phys. **114**, 1754,1763,5682 (2001).
- <sup>18</sup>A. I. Burshtein and P. A. Frantsuzov, J. Chem. Phys. **106**, 3948 (1997).
- <sup>19</sup>R. A. Marcus, J. Chem. Phys. **24**, 966 (1956); R. A. Marcus, Annu. Rev. Phys. Chem. **15**, 155 (1964).
- <sup>20</sup>A. I. Burshtein and P. A. Frantsuzov, Chem. Phys. **212**, 137 (1996).
- <sup>21</sup>A. I. Burshtein and E. B. Krissinel, J. Phys. Chem. **100**, 3005 (1996).
- <sup>22</sup>A. I. Burshtein, I. V. Gopich, and P. A. Frantsuzov, Chem. Phys. Lett. **289**, 60 (1998).
- <sup>23</sup>D. Rehm and A. Weller, Isr. J. Chem. **8**, 259 (1970); N. Mataga, T. Asahi, Y. Kanda, and T. Okada, Chem. Phys. **127**, 249 (1988); F. Lewitzka and H.-G. Löhmannsröben, Z. Phys. Chem., Neue Folge **169**, 181 (1990); E. Vauthey, J. Phys. Chem. A **105**, 340 (2001).
- <sup>24</sup>C. G. Kavakatsanis and T. B. Reddy, in *IUPAC, Anal. Chem. Div.*, "Recommended Methods for Purification of Solvents and Tests for Impurities," edited by J. F. Coetzee (Pergamon, Oxford, 1982), p. 25.
- <sup>25</sup>G. Angulo, G. Grampp, and S. Landgraf, J. Inf. Rec. **25**, 381 (2000).